Journal of Environmental Radioactivity 152 (2016) 16–22

Contents lists available at ScienceDirect

Journal of Environmental Radioactivity

journal homepage: www.elsevier.com/locate/jenvrad

Study of water mixing in the coastal waters of the western Taiwan Strait based on radium isotopes

Wu Men [a, *], Yuwu Jiang [b], Guangshan Liu [b], Fenfen Wang [a], Yusheng Zhang [a]

[a] Laboratory of Marine Isotopic Technology and Environmental Risk Assessment, Third Institute of Oceanography, State Oceanic Administration, Xiamen 361005, PR China
[b] State Key Laboratory of Marine Environmental Science, Xiamen University, Xiamen 361005, PR China

ARTICLE INFO

Article history:
Received 28 March 2015
Received in revised form
8 November 2015
Accepted 8 November 2015
Available online xxx

Keywords:
Radium isotopes
Water mixing
Residence time

ABSTRACT

Radium is considered to be a useful tracer for studying the physical processes of seawater. In this work, three naturally occurring radium isotopes, $^{224}Ra_{ex}$, ^{226}Ra and ^{228}Ra, were measured in the coastal zone of the western Taiwan Strait during the summer seasons. Based on the distributions of the three radium isotopes and the salinity, we conclude that the water mixing pattern in the study area in summer consists of diluted water flowing from the Jiulong River to the open sea towards the east and southeast, and open sea seawater flowing inward from south to north. The submarine ground water discharges in the estuarine region, as suggested by the radium and salinity data. The residence times of the Jiulong River estuary, ranging from 7 to 49 d, were estimated using the radium isotope pairs $^{224}Ra_{ex}$ and ^{226}Ra.

1. Introduction

The exchange of material between the continental margin and the open sea plays a key role in global biogeochemical cycling. Physical mixing in estuaries and the coastal ocean is responsible for the dispersion of land-based anthropogenic inputs (e.g., nutrients and pollutants), sediment-generated nutrients and metals, as well as algal blooms, plumes and spills (Torgersen et al., 1996). The processes of physical mixing, which include advection and diffusion, are integral to the understanding of the exchange and transport of material at the land–sea interface. The eddy diffusion coefficient and advection velocity are the most important parameters in physical oceanography and are used to express the rates of the eddy diffusion and advection, respectively. However, these parameters are difficult to quantify because these systems are exceedingly complex due to their small-scale temporal and spatial variability. Chemical tracers offer promise but few techniques have been developed to study this complex region. However, naturally occurring radium isotopes provide a useful tool for the study of these marine processes (Moore, 2000).

Four radium isotopes, ^{223}Ra, ^{224}Ra, ^{226}Ra and ^{228}Ra, are delivered to the ocean by river inputs, bottom sediment inputs and submarine ground water discharge (SGD). Radium isotopes are soluble and preserved in seawater. Consequently, they can be used individually as tracers or in pairs to study ocean-mixing processes. Radium-226 ($t_{1/2} = 1602$ y) is a suitable tracer for marine processes with time scales of a thousand years. Radium-228 ($t_{1/2} = 5.75$y) is a valuable natural tracer of water mixing on the order of 1–30 y but is of little use in delineating relatively short-term processes. Radium-224 ($t_{1/2} = 3.66$ d) is a useful tracer for marine processes that occur within a 1- to 10-dscale. Radium-223 ($t_{1/2} = 11.4$ d) is another useful tracer for marine processes that occur within several weeks. In coastal waters and the open sea, radium isotopes have been used to provide important information about mixing processes, including diffusion (Moore, 2000; Rengarajan et al., 2002), pore-water and surface water exchange (Bollinger and Moore, 1993; Webster et al., 1994), water transport rates (Turekian et al., 1996; Turekian et al., 1996) and groundwater outflow (Rama and Moore, 1996; Krest and Harvey, 2003).

The Taiwan Strait, the channel connecting the South China Sea and the East China Sea, is located between mainland China and Taiwan Island. The Jiulong River, the second largest river in the Fujian province, discharges into the coastal area of the western Taiwan Strait, with an annual average river flow of 1.48×10^{10} m^3; it is the major source of freshwater to the coastal area. The geographical setting determines that this area receives wastewater with high nutrient and pollutant loading from both the Jiulong River catchment and urban (Xiamen City) sewage (Cao et al., 2005).

* Corresponding author.
E-mail address: men_wu@126.com (W. Men).

http://dx.doi.org/10.1016/j.jenvrad.2015.11.003
0265-931X/

Since the mid-1980s, eutrophication and the excessive growth of benthic algae, which causes a deterioration in the quality of seawater, have accelerated in the Jiulong estuary and coastal ocean (Chen et al., 1993; Hong et al., 1999). Thus, many physical, chemical and biological studies have focused on the fate of these nutrients and pollutants. In this work, the mixing processes in the western Taiwan Strait were studied and the residence times of the surface seawater of Jiulong River estuary were estimated using radium isotopes.

2. Sampling and methods

2.1. Sampling stations

Water samples were collected in June 2009 on the "Yanping 2" vessel. The sampling period is typical of summer conditions. The temperature of the seawater is high with ~24–~28 °C. The sampling stations and detailed information are shown in Fig. 1 and Table 1. There are 34 stations distributed in transects A–F. Vertical sampling was performed at stations A5, B2, C3, D4, and E6. All other stations were surface sampling stations.

All the errors in this table were calculated using an error transfer formula, including counting error, background error and efficiency error.

2.2. Sampling and analysis

Approximately 70 L of seawater was pumped and collected into a plastic container. The seawater was pumped sequentially through the flowmeter, then columns A, B and C at the rate of ~400 mL/min. Column A was used to filter suspended solids. Column B and column C were MnO_2-fiber columns with12 g MnO_2-fiber inside. Column B was used to determine the activities of the radium isotopes in the seawater, and column C was used to determine the extracting efficiency. A previous study showed that greater than 99% of radium isotopes could be extracted by the 12 g MnO_2-fiber at a seawater flow rate of less than 500 mL/min (Chen et al., 2011). After sampling, the sample fibers were carefully shaken to remove water and were stored in plastic bags for the measurement of the radium isotopes.

Radium-224 activity was measured by the ^{220}Rn emanation method (Men et al., 2013). After sampling, the samples were shaken to remove water. Nitrogen gas was introduced to carry the original ^{220}Rn and ^{222}Rn in the MnO_2-fiber sample column out of the measurement system over the first 5 min and then to carry the ^{220}Rn that emanated from the samples into the Rn–Th analyzer (FD-125, Beijing Nuclear Instrument Factory, Beijing, China) to determine the ^{224}Ra activity (Fig. 2). With a very short half-life of 55.6 s, ^{220}Rn can reach equilibrium with ^{224}Ra in several minutes. The ^{222}Rn emanating from ^{226}Ra does not interfere with the measurement of ^{220}Rn. A standard of ^{232}U–^{228}Th–^{224}Ra (A11416, National Physical Laboratory, UK) in equilibrium was used to determine the efficiency of the measurement system.

The level of ^{224}Ra supported by its parent ^{228}Th was corrected using separate measurements. After the first measurements were complete, the MnO_2-fiber samples were aged for approximately 6 weeks to allow for the supported ^{224}Ra to equilibrate with ^{228}Th absorbed onto the MnO_2-fiber. The samples were measured again to determine the ^{224}Ra supported by ^{228}Th. The differences between the two measurement results are the excess ^{224}Ra activities ($^{224}Ra_{ex}$), which are reported in this paper.

The ^{226}Ra activity was measured using the ^{222}Rn emanation method (Yang et al., 2007). Briefly, the MnO_2-fiber was removed from the plastic bag and placed into a diffusion tube, which was sealed and evacuated. After 5–20 d, when the ingrown ^{222}Rn reached a significant level, the ^{222}Rn was introduced into an evacuated scintillation counting cell. After being sealed in the cell for 3 h until reaching an equilibrium of ^{222}Rn with its daughters, their activities were measured using the Rn–Th analyzer. A ^{226}Ra standard (GBW04312, National Institute of Metrology, China) was used to determine the efficiency of the measurement system.

The MnO_2-fibers were then stored for more than 1 y after the measurement of ^{226}Ra, after which the ^{228}Ra activity was measured through determining the ^{224}Ra growing from ^{228}Ra by the aforementioned method.

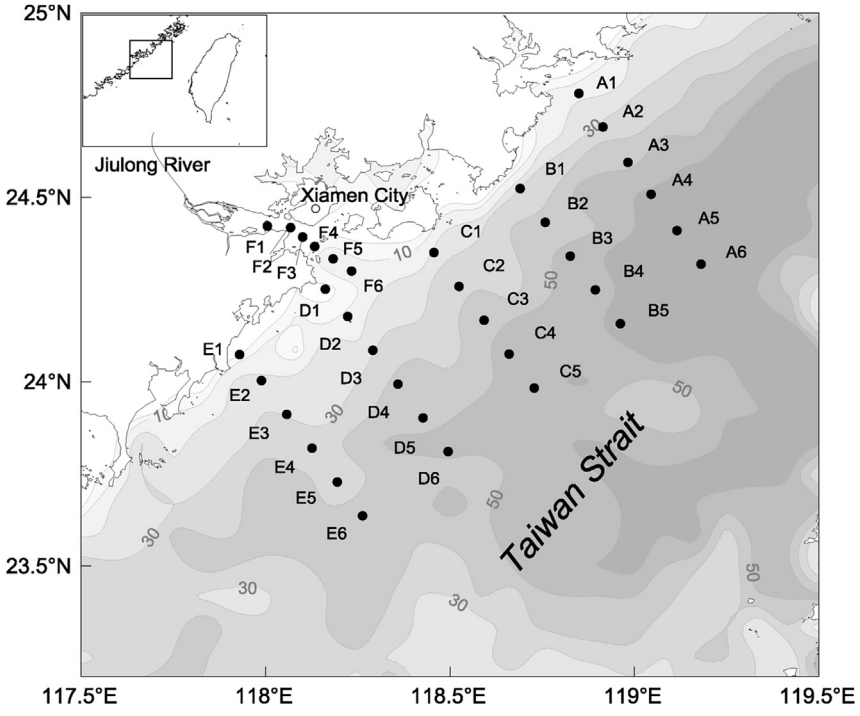

Fig. 1. Map of sampling stations with the isobaths.

Table 1
Data of radium isotopes, salinity, temperature and stations.

Station	Longitude	Latitude	Layer	T (°C)	S (‰)	$^{224}Ra_{ex}$	^{226}Ra	^{228}Ra
	(°E)	(°N)	(m)			(Bq/m^3)		
F1	118.0051	24.4221	0	27.98	21.48	21.2 ± 1.7	5.82 ± 0.51	12.1 ± 1.2
F2	118.0680	24.4180	0	27.9	25.42	20.9 ± 1.7	6.97 ± 0.59	24.1 ± 2.3
F3	118.1333	24.3667	0	27.54	30.84	15.3 ± 1.2	3.31 ± 0.31	11.9 ± 1.2
F4	118.1007	24.3924	0	27.79	27.48	17.4 ± 1.4	4.98 ± 0.44	11.9 ± 1.1
F5	118.1833	24.3333	0	27.39	33.17	8.61 ± 0.69	2.30 ± 0.23	6.50 ± 0.68
F6	118.2333	24.3000	0	27.35	33.13	7.25 ± 0.58	2.76 ± 0.28	5.81 ± 0.61
A1	118.8495	24.7818	0	26.59	33.64	3.35 ± 0.27	1.69 ± 0.19	7.10 ± 0.84
A2	118.9147	24.6907	0	26.8	33.59	2.36 ± 0.19	1.52 ± 0.17	5.34 ± 0.58
A3	118.9824	24.5946	0	27.97	33.04	2.04 ± 0.16	2.10 ± 0.23	8.26 ± 0.88
A4	119.0452	24.5084	0	27.05	33.39	2.03 ± 0.16	1.89 ± 0.20	5.12 ± 0.56
A5	119.1153	24.4099	0	25.11	34.06	0.60 ± 0.05	1.70 ± 0.18	5.19 ± 0.60
A6	119.1806	24.3188	0	28.03	33.52	0.81 ± 0.06	1.67 ± 0.19	1.82 ± 0.23
			10	27.87	33.56	0.83 ± 0.07	1.60 ± 0.18	3.19 ± 0.38
			20	27.57	33.56	0.65 ± 0.05	1.50 ± 0.16	3.01 ± 0.40
			30	25.37	34.85	0.96 ± 0.08	1.45 ± 0.17	1.98 ± 0.31
			40	25.00	34.21	1.89 ± 0.15	1.42 ± 0.17	1.71 ± 0.23
			50	25.00	34.11	2.86 ± 0.23	1.62 ± 0.16	2.47 ± 0.33
B1	118.6903	24.5238	0	26.66	33.35	3.51 ± 0.28	1.96 ± 0.21	7.06 ± 0.77
B2	118.7582	24.4322	0	27.45	32.88	3.33 ± 0.27	2.18 ± 0.23	8.53 ± 0.86
			10	26.57	33.32	1.39 ± 0.11	1.99 ± 0.21	4.49 ± 0.53
			20	26.31	33.41	1.58 ± 0.13	1.89 ± 0.20	3.96 ± 0.42
			30	25.76	33.87	1.45 ± 0.12	1.77 ± 0.17	2.71 ± 0.35
			40	25.7	33.90	2.31 ± 0.19	1.47 ± 0.17	2.06 ± 0.34
			47	25.7	33.90	2.95 ± 0.24	1.47 ± 0.18	2.94 ± 0.44
B3	118.8261	24.3405	0	27.03	33.44	1.52 ± 0.12	1.61 ± 0.17	3.78 ± 0.44
B4	118.8940	24.2489	0	27.53	33.49	1.57 ± 0.13	1.53 ± 0.17	2.62 ± 0.30
B5	118.9619	24.1572	0	27.62	33.34	0.57 ± 0.05	1.54 ± 0.17	3.51 ± 0.39
C1	118.4566	24.3503	0	28.35	31.94	9.43 ± 0.75	2.97 ± 0.29	11.71 ± 1.14
C2	118.5245	24.2584	0	27.00	33.30	6.15 ± 0.49	1.79 ± 0.19	8.95 ± 0.99
C3	118.5925	24.1666	0	26.90	33.35	1.43 ± 0.11	1.41 ± 0.16	3.09 ± 0.37
			10	26.88	33.37	1.23 ± 0.10	1.43 ± 0.18	4.33 ± 0.48
			20	26.64	33.41	1.42 ± 0.11	1.67 ± 0.18	3.62 ± 0.44
			30	26.46	33.51	1.03 ± 0.08	1.56 ± 0.18	3.23 ± 0.41
			40	26.21	33.76	1.76 ± 0.14	1.40 ± 0.17	2.28 ± 0.25
			47	26.12	33.79	1.99 ± 0.16	1.23 ± 0.15	1.52 ± 0.21
C4	118.6604	24.0748	0	27.27	33.27	1.67 ± 0.13	1.39 ± 0.16	5.77 ± 0.65
C5	118.7284	23.9829	0	27.47	33.33	0.93 ± 0.07	1.48 ± 0.17	3.92 ± 0.48
D1	118.1621	24.2509	0	27.36	33.14	5.64 ± 0.45	2.15 ± 0.22	5.75 ± 0.70
D2	118.2228	24.1767	0	26.09	33.31	3.75 ± 0.30	1.93 ± 0.21	5.60 ± 0.54
D3	118.2909	24.0851	0	26.16	33.33	2.62 ± 0.21	1.82 ± 0.18	5.23 ± 0.60
D4	118.3589	23.9935	0	26.71	33.32	2.67 ± 0.21	1.94 ± 0.21	5.04 ± 0.55
			10	25.59	33.48	2.95 ± 0.24	1.78 ± 0.19	3.73 ± 0.40
			20	24.62	33.59	1.85 ± 0.15	1.67 ± 0.19	4.07 ± 0.44
			30	24.56	33.59	2.99 ± 0.24	1.20 ± 0.16	5.04 ± 0.57
			40	24.55	33.59	3.43 ± 0.27	1.91 ± 0.19	6.06 ± 0.70
D5	118.4269	23.9019	0	26.69	33.41	2.56 ± 0.20	1.79 ± 0.21	4.53 ± 0.49
D6	118.4949	23.8104	0	26.32	33.41	2.51 ± 0.20	1.90 ± 0.21	4.45 ± 0.47
E1	117.9297	24.0733	0	25.73	33.41	4.50 ± 0.36	1.94 ± 0.20	6.86 ± 0.83
E2	117.9891	24.0031	0	26.19	33.38	5.09 ± 0.41	1.86 ± 0.20	6.10 ± 0.74
E3	118.0576	23.9114	0	26.46	33.41	3.86 ± 0.31	1.89 ± 0.20	5.90 ± 0.66
E4	118.1261	23.8196	0	26.04	33.25	2.58 ± 0.21	1.80 ± 0.19	5.50 ± 0.66
E5	118.1946	23.7278	0	26.73	33.08	2.36 ± 0.19	2.12 ± 0.20	6.73 ± 0.72
E6	118.2631	23.6361	0	27.26	32.97	2.02 ± 0.16	1.98 ± 0.20	2.81 ± 0.38
			10	27.04	32.97	1.91 ± 0.15	1.53 ± 0.17	3.62 ± 0.41
			20	26.99	32.97	2.34 ± 0.19	1.88 ± 0.19	6.23 ± 0.76
			30	26.99	33.01	2.64 ± 0.21	1.88 ± 0.19	4.33 ± 0.58
			40	26.79	33.13	2.92 ± 0.23	1.95 ± 0.20	4.27 ± 0.48
Average				26.65	32.93	3.82	2.02	5.43
Range				24.65–28.35	21.45–34.85	0.57–21.2	1.20–6.97	1.52–24.1

All of the measurement results were corrected for the extracting efficiency, sample volume and sampling time. A typical single standard deviation from the counting statistics for the radium isotope activities was ~8%.

3. Results

3.1. Concentrations of $^{224}Ra_{ex}$, ^{226}Ra and ^{228}Ra

The concentrations of $^{224}Ra_{ex}$, ^{226}Ra and ^{228}Ra are listed in Table 1. As shown in Table 1, the $^{224}Ra_{ex}$ concentrations varied from 0.57 to 21.2 Bq/m^3, with an average of 3.82 Bq/m^3. The ^{226}Ra and ^{228}Ra concentrations varied from 1.02 Bq/m^3 to 6.97 Bq/m^3 with an average of 2.02 Bq/m^3, and from 1.52 Bq/m^3 to 24.1 Bq/m^3 with an average of 5.43 Bq/m^3, respectively.

3.2. Horizontal distribution of radium isotope concentrations

Contour maps of the $^{224}Ra_{ex}$, ^{226}Ra and ^{228}Ra concentrations in the surface seawater samples are given in Fig. 3, showing that the

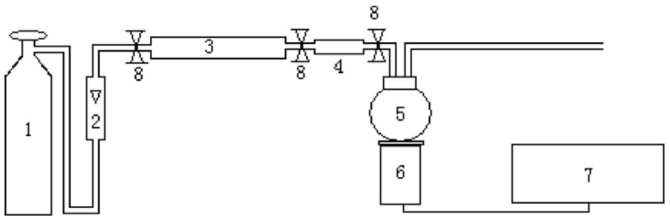

Fig. 2. Schematic measurement equipment of ^{224}Ra. 1. N_2 gas cylinder; 2. Flow meter; 3. MnO_2-fiber sample column; 4. Drying tube; 5. Scintillation cell; 6. Photomultiplier and pre-amplifier (5 and 6 constitute the detector); 7. Scaler; 8. Gas valves.

distribution features of the radium isotopes concentrations were similar to each other. Nearly all of the distribution transects showed that higher radium activities were observed at the shoreline and decreased with the offshore distance (Table 1). With subsequent water mixing, the level of the radium isotopes gradually decreased.

3.3. Relationship of radium isotope concentrations with salinity and temperature

The contour map of salinity in the surface seawater in the study area is shown in Fig. 4. The distribution pattern of salinity is obviously similar with that of each $^{224}Ra_{ex}$, ^{226}Ra, and ^{228}Ra concentration (Fig. 3). The x-y plotting of salinity and Ra isotopes is given in Fig. 5, which demonstrates that the salinity was negatively correlated with the each Ra isotope. It suggests that the distributions of these four components are dominated by the same seawater mixing mechanism and are controlled by mixing between fresh water and open seawater. The shape of the contour lines demonstrates the mixing mode of surface seawater in the study sea area. The surface seawater from the open sea flows towards the shore from south to north (in the direction shown by the dotted arrow in Fig. 3), and diluted Jiulong River water flows offshore towards the east and southeast (in the direction shown by the solid arrow in Fig. 3).

The x-y plotting of temperature and radium isotopes is shown in Fig. 6. There are no correlations among them.

3.4. Vertical distribution of $^{224}Ra_{ex}$ concentration

The vertical distributions of the $^{224}Ra_{ex}$ concentration at the aforementioned stations are shown in Fig. 7. Two distribution patterns were observed: (1) at stations B2, C3 and D4, the activity of $^{224}Ra_{ex}$ in the surface or upper layer and near-bottom layer was higher than that of the middle layer, suggesting that $^{224}Ra_{ex}$ is derived not only from the upward diffusion of interstitial water from sediments but also from lateral input; (2) at stations A5 and E6, the activity of $^{224}Ra_{ex}$ increased with increasing depth, suggesting that $^{224}Ra_{ex}$ is mainly derived from the upward diffusion of interstitial water from sediments.

4. Discussion

4.1. Evidence of SGD

Transect F was located between the Jiulong River estuarine and the open sea area (Fig. 1). As shown in Table 1, the activities of $^{224}Ra_{ex}$, ^{226}Ra and ^{228}Ra of stations F1 to F6 decreased with the increasing distances from the estuarine except for station F4, which suggested that there was a new source of radium activity at station F4. Moreover, the salinities of stations F1 to F6 increased with the decreasing distances from the open sea except for station F4, which suggests that there was a low-salinity water body input at station

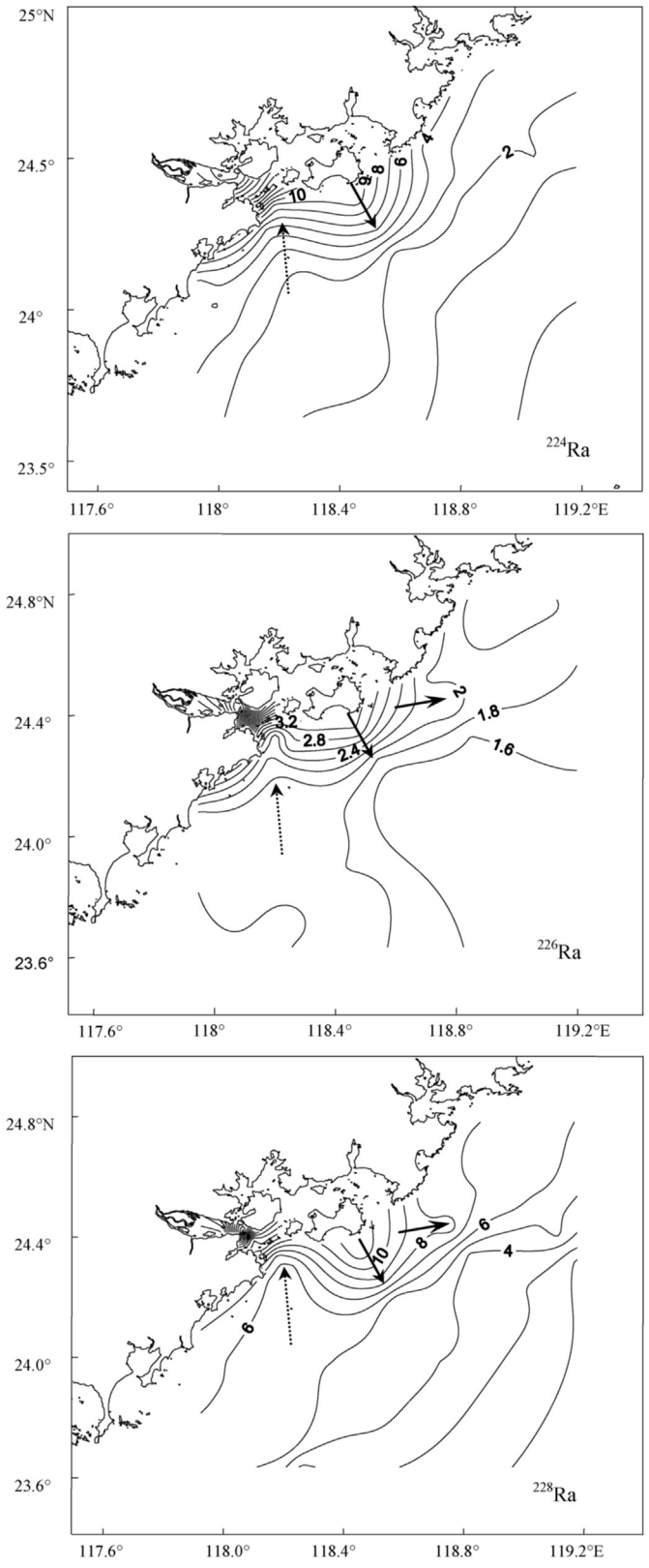

Fig. 3. Distribution of $^{224}Ra_{ex}$, ^{226}Ra and ^{228}Ra concentrations in surface seawater (Bq/m^3). The dotted arrows indicate the direction of the surface seawater flow in and the solid arrows indicate the direction of diluted Jiulong River water flow in.

F4. There are two possible reasons for this characteristic of lower salinity and higher radium concentration: river discharge or SGD. As there is no river discharge in this area, it indicates that

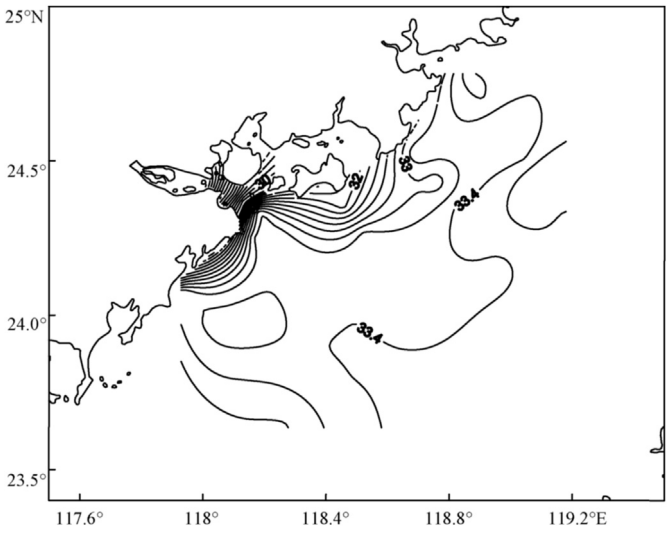

Fig. 4. Salinity distribution of the study area (‰).

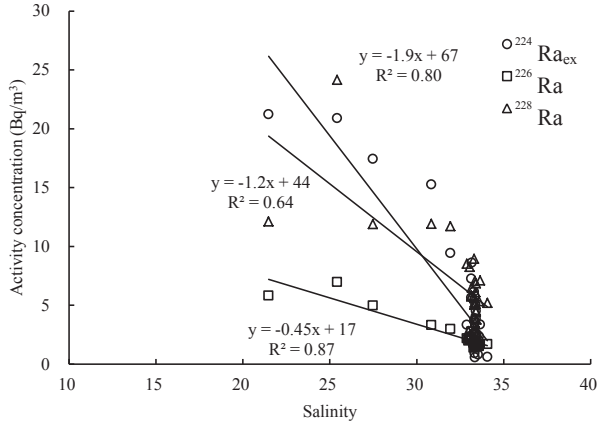

Fig. 5. The correlation between salinity and concentration of $^{224}Ra_{ex}$, ^{226}Ra and ^{228}Ra in surface seawater.

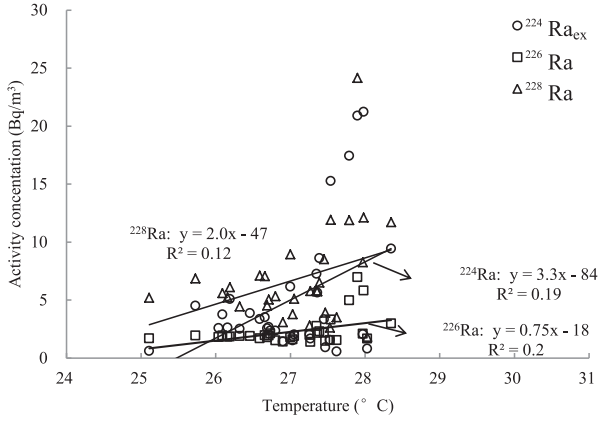

Fig. 6. The correlation between temperature and the concentrations of radium isotopes.

submarine groundwater discharge may occur in this area. Unfortunately, due to a lack of necessary data of the fresh water end member, the sediment end member and the groundwater end member, we cannot evaluate the SGD flux based on the current data.

4.2. The residence time of the surface water in Jiulong River estuary

As an important topic of marine environment research, the residence time of water determines the speed at which pollutants can be flushed out of a water body and further evaluations of the behavior and fates of substances or biota. It is frequently used as an independent variable when processes and biogeochemical properties are studied. Radium can be used to estimate the residence time of the shelf area (Nozaki et al., 1991; Lee et al., 2005). Radium has three potential sources in shelf water: (1) Ra_R, radium from the riverine freshwater end-member; (2) Ra_S, radium from the open sea; and (3) Ra'_{ex}, excess radium that is newly supplied to the water on the shelf due to the combined effects of diffusion from sediments, desorption from suspend particles, biological uptake/release, SGD, and radioactive decay. Therefore, the chemical mass balance for $^{224}Ra_{ex}$, ^{226}Ra and ^{228}Ra is given by the following equations:

$$^{224}Ra_{ex} = f^{224}Ra_{ex\,S} + (1-f)^{224}Ra_{ex\,R} + {}^{224}Ra'_{ex} \quad (1)$$

$$^{226}Ra = f^{226}Ra_S + (1-f)^{226}Ra_R + {}^{226}Ra'_{ex}, \quad (2)$$

where f is the fraction of the open sea end-member. Assuming that the shelf water at a salinity of S represents a mixture of the riverine freshwater and the open seawater and that the net effect of evaporation and precipitation is negligible, we obtain the following:

$$f = \frac{S}{S_S} \quad (3)$$

where S_S is the salinity of the open sea water.

For ^{226}Ra,

$$^{226}Ra'_{ex} = (I_{226} - \lambda_{226}\,{}^{226}Ra)\tau. \quad (4)$$

Because the decay of ^{226}Ra is negligible, $^{226}Ra'_{ex}$ at steady state may be expressed as:

$$^{226}Ra'_{ex} = I_{226}\tau, \quad (5)$$

where I_{226} is the total flux of $^{226}Ra'_{ex}$ (neglecting the effect of biological activity), and τ is the mean residence time of the shelf water.

Similarly, $^{224}Ra'_{ex}$ can be expressed as follows;

$$^{224}Ra'_{ex} = (I_{224} - \lambda_{224}\,{}^{224}Ra_{ex})\tau, \quad (6)$$

where I_{224} is the total flux of ^{224}Ra due to the same effect as for ^{226}Ra, and λ_{224} is the decay constant of ^{224}Ra. Dividing Eq. (6) by Eq. (5) gives:

$$\frac{^{224}Ra'_{ex}}{^{226}Ra'_{ex}} = \frac{I_{224}}{I_{226}} - \frac{\lambda_{224}}{I_{226}}\,{}^{224}Ra_{ex} \quad (7)$$

the least-squares fitting of the $^{224}Ra'_{ex}/^{226}Ra'_{ex}$ and $^{224}Ra_{ex}$ Eq. (7) gives λ_{224}/I_{226} as the slope of the regression line. Then, the I_{226} can be deduced. Further, the residence time at each station can be calculated by Eq. (5).

According to the method mentioned above, the residence time of surface water was estimated based on the data obtained in this study. According to the salinity distributions, transect F, which is located in the Jiulong River estuary, is the most suitable for estimating the residence time. By choosing the isotope pairs $^{226}Ra/^{224}Ra_{ex}$ and the end-member values for river and open seawater (Table 2), Eq. (7) were fitted as Fig. 8. The coefficient of determination (R^2) is 0.90, which illustrates a well fit between

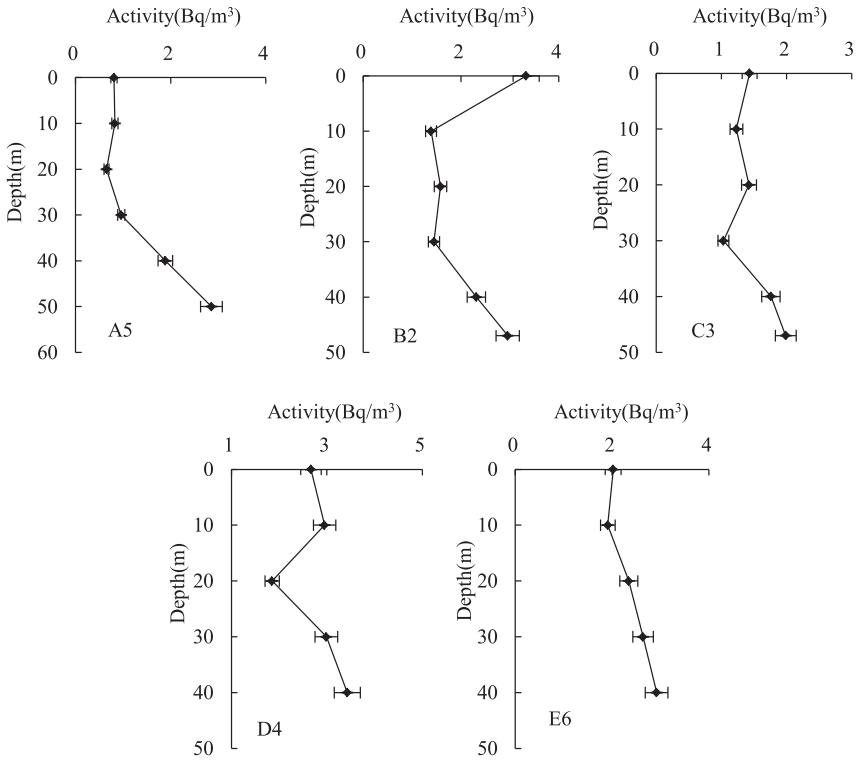

Fig. 7. Vertical distribution of $^{224}Ra_{ex}$.

these two parameters, and the standard error of the slope was 9.6%. The residence time of the surface water of the Jiulong River estuary was estimated to range from 7 to 49 d (Table 3) with an average of 28 d. The errors in the Table 3 were propagated from the errors of the least-squares fitting and the $^{224}Ra'_{ex}$ concentration. These results suggest that non-reactive pollutants, such as alkaline and alkali earth elements, remain in Jiulong River estuary for approximately 28 d on average. Because we collected the surface waters during a period of high discharge, the estimated residence time values could reach the upper limit during summer, and the actual mean values of the residence time could be lower than our estimates. Our estimated results are comparable to the results in the other coastal sea areas of 5–42 d (Kasemsupaya et al., 1989; Moore, 1997; Lee et al., 2005).

The calculated residence times in this work decreased toward the open sea. The same situation was found in the Ulsan Bay (Lee et al., 2005), the waters in the upper part of the estuary of the Ulsan Bay have long residence times, whereas those in the lower part, in contact with the open sea, have shorter residence times.

5. Conclusions

In this study, we used ^{224}Ra, ^{226}Ra and ^{228}Ra to study the mixing rates in the coastal zone of the western Taiwan Strait during the summer season. Some physical oceanography issues were addressed from an isotopic oceanography perspective. The water-mixing pattern in the study area in summer was demonstrated that the Jiulong River-diluted water flows to the open sea eastward and southeastward, and the open seawater flows inward from south to north. The residence time of the internal water ranging from 7 to 49 d was also estimated using the radium isotope pairs ^{224}Ra and ^{226}Ra. In addition, the radium and salinity data suggested that the submarine ground water discharge occurred in the

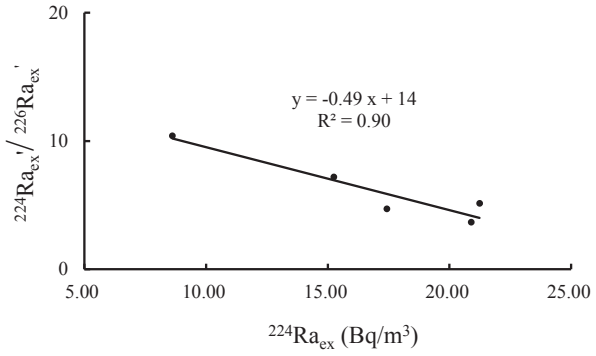

Fig. 8. The least-squares fitting of the $^{224}Ra'_{ex}/^{226}Ra'_{ex}$ and $^{224}Ra_{ex}$.

Table 3
The Residence time of internal water.

Station	$^{226}Ra_{ex}$ (Bq/m^3)	I_{226} (Bq/m^3/d)	Residence time (d)
F1	3.55	0.10	34 ± 2
F2	5.09	0.10	49 ± 2
F3	1.95	0.10	19 ± 1
F4	3.30	0.10	32 ± 2
F5	0.75	0.10	7 ± 1
Average			28

Table 2
Values of different end-members.

	River end-member	Open sea end-member	Reference
Salinity	0	34.5	Xie, 1994
$^{224}Ra_{ex}$	7.1Bq/m^3	0.50 Bq/m^3	Men et al., 2011
^{226}Ra	4.36 Bq/m^3	1.00 Bq/m^3	Huang, 2006

estuarine area (station F4). The work in this study demonstrates that the radium isotope tracer technique is an effective method for use in further studies of water mixing.

Acknowledgments

This study was conducted as part of the China national project of the IAEA/RCA RAS/7/024and was supported by the Project supported by the National Science Foundation for Distinguished Young Scholars of China (Grant No. 41006044), the Scientific Research Foundation of Third Institute of Oceanography, State Oceanic Administration under contact No.TIO 2009050, and by Natural Science Foundation of Fujian Province (No.2012J05077) as well as the Science and Technology Program of Xiamen (No.3502Z20132007) We thank the IAEA/RCA for providing training on nuclear analytical techniques relevant to the project activities.

References

Bollinger, M.S., Moore, W.S., 1993. Evaluation of salt marsh hydrology using radium as a tracer. Geochim. Cosmochim. Ac 57, 2203–2212.
Cao, W.Z., Hong, H.S., Yue, S.P., 2005. Modelling agricultural nitrogen contributions to the Jiulong River estuary and coastal water. Glob. Planet. Change 47, 111–121.
Chen, M., Li, Y.P., Qiu, Y.S., Yang, J.H., 2011. Water masses in the Bering Strait revealed by radium isotopes. Acta Oceanol. Sin. 33 (2), 69–76 (in Chinese).
Chen, S.T., Ruan, W.Q., Zhen, R.Z., 1993. The biogeochemical study of phosphorus in the Jiulong River estuary and Western Sea. Acta Oceanol. Sin. 15 (1), 62–70 (in Chinese).
Hong, H., Shang, S., Huang, B., 1999. An estimate on external fluxes of phosphorus and its environmental significance in Xiamen Western Sea. Mar. Pollut. Bull. 39, 200–204.
Huang, L., 2006. Research on Groundwater Discharge into Jiulongjiang Estuary. Master thesis(in Chinese). Xiamen University.
Kasemsupaya, V., Yashima, M., Tsubota, H., Nozaki, Y., 1989. Comparative behavior of ^{210}Pb and Ra isotopes in the waters of Tokyo Bay and Osaka Bay mixing zones. Geochem. J. 23, 129–138.
Krest, J.M., Harvey, J.W., 2003. Using natural distributions of short-lived radium isotopes to quantify groundwater discharge and recharge. Limno. Oceanogr. 48 (1), 290–298.
Lee, J.S., Kim, K.H., Moon, D.S., 2005. Radium isotopes in the Ulsan Bay. J. Environ.Radioact. 82, 129–141.
Men, W., Wang, F.F., Liu, G.S., 2011. ^{224}Ra and its implications in the East China Sea. J. Radioanal. Nucl. Ch 288, 189–195.
Men, W., Wang, F.F., Zhang, Y.S., He, J.H., Yu, W., Li, Y.L., 2013. Determining coastal mixing rates of western Taiwan Strait using ^{224}Ra. J. Radioanal. Nucl. Ch. 295, 89–94.
Moore, W.S., 1997. High fluxes of radium and barium from the mouth of the Gangese Brahmaputra River during low river discharge suggest a large groundwater sources. Earth. Planet. Sc. Lett. 150, 141–150.
Moore, W.S., 2000. Determining coastal mixing rates using radium isotopes. Cont. Shelf Res. 20, 1993–2007.
Nozaki, Y., Tsubota, H., Kasemsupaya, V., Yashima, M., Ikuta, N., 1991. Residence times of surface water and particle reactive^{210}Pb and ^{210}Po in the East China and Yellow seas. Geochim. Cosmochim. Ac 55, 1265–1272.
Rama, Moore, W.S., 1996. Using the Ra quartet for evaluating groundwater input and water exchange in salt marshes. Geochim. Cosmochim. Ac 60, 4645–4652.
Rengarajan, R., Sarin, M.M., Somayajulu, B.L.K., Suhasini, R., 2002. Mixing in the surface waters of the western Bay of Bengal using ^{228}Ra and ^{226}Ra. J. Mar. Res. 60, 255–279.
Torgersen, T., Turekian, K.K., Turekian, V.C., Tanaka, N., Deangelo, E., O'Donnell, J., 1996. ^{224}Ra distribution in surface and deep water of Long Island Sound: sources and horizontal transport rates. Cont. Shelf Res. 16 (12), 1545–1559.
Turekian, K.K., Tanaka, N., Turekian, V.C., Torgensen, T.E., Deangelo, E.C., 1996. Transfer rates of dissolved tracers through estuaries based on ^{228}Ra: a study of Long Island Sound. Estuar. Coast. Shelf S 16, 863–873.
Webster, I.T., Hancock, G.J., Murry, A.S., 1994. On the use of radium isotopes to examine pore water exchange in an estuary. Limno. Oceanogr. 39, 1917–1927.
Xie, Y.Z., 1994. A Study on Radium Isotopes Geochemical in South China Sea and Xiamen Adjacent Sea Area (Doctor thesis). Xiamen University.
Yang, J.H., Chen, M., Qiu, Y.S., Li, Y.P., Ma, Q., Lv, E., Huang, Y.P., 2007. ^{226}Ra evidence for the ecosystem shift over the past 40 y in the North Pacific Subtropical Gyre. Chin. Sci. Bull. 52 (6), 832–838.